Linked Lexitropsins and the *in Vitro* Inhibition of HIV-1 Reverse Transcriptase RNA-Directed DNA Polymerization: A Novel Induced-Fit of 3,5 *m*-Pyridyl Bisdistamycin to Enzyme-Associated Template-Primer[†]

Mark E. Filipowsky, Mary L. Kopka,* Michelle Brazil-Zison, J. William Lown,[‡] and Richard E. Dickerson

Molecular Biology Institute, University of California at Los Angeles, Los Angeles, California 90095

Received July 2, 1996; Revised Manuscript Received September 10, 1996[⊗]

ABSTRACT: Five classic DNA minor groove-binding drugs and a series of bis-linked lexitropsins based on netropsin and distamycin have been screened for their effectiveness in inhibiting transcription by HIV-1 reverse transcriptase (RT) on a poly(rA)·oligo(dT) template−primer (TP). The two most effective drugs, 3,5 *m*-pyridyl-linked bisdistamycin (MPyr) and *trans*-vinyl-linked bisdistamycin (TVin), show (1) enhanced inhibition in reactions initiated with pre-incubated enzyme template-primer (ETP) and (2) reduced affinity for a "free" TP analog, when compared with the parent drug distamycin. All three drugs lack the ability to inhibit processive incorporation of nucleotide, suggesting drug intervention instead at initiation or termination of processive cycles. The two bis-linked drugs exhibit different kinetic behavior with reverse transcriptase's two substrates: template−primer and nucleotide. When primer is the variable substrate, TVin is partially noncompetitive and MPyr is dead-end competitive ($K_i = 6.5$ μM). With nucleotide as substrate, TVin is noncompetitive at low drug concentrations and MPyr is uncompetitive. Gel band mobility shift assays with MPyr indicate that the drug inhibits via entrapment of TP on the enzyme rather than displacement of TP from the enzyme surface. The conformation of nucleic acid is most likely altered upon MPyr binding, enhancing the induced fit of enzyme to hybrid duplex. The relevance of this novel mode of inhibition is considered in relation to enzyme association/dissociation with TP that occurs prior to (−)-DNA strand transfer, and to the structural implications of an enzyme-bound hybrid RNA/DNA nucleic acid.

The naturally occurring oligopeptide antibiotics netropsin and distamycin (Zimmer & Luck, 1970; Zimmer et al., 1971a,b; Wartell et al., 1974) are well-known for their strong affinity for DNA. They bind within the minor groove of B-DNA at sites consisting of four or five consecutive AT base pairs, respectively (Patel, 1982; Kopka et al., 1985a,b). It has been demonstrated *in vitro* that these compounds inhibit many DNA-dependent enzymatic functions associated with DNA replication or RNA transcription. Enzymes affected include DNA and RNA polymerases and topoisomerases (Puschendorf & Grunicke, 1969; Zimmer et al., 1971b; Wahnert et al., 1975; Woynarowski et al., 1989; Mortensen et al., 1990; McHugh et al., 1990; Ueno et al., 1992), as well as DNA gyrase and helicase (Bachur et al., 1993; Storl et al., 1993). Recent studies, moreover, have illustrated the ability of these groove-binding drugs to prevent the binding of transcription factors (Gambari et al., 1991; Dorn et al., 1992; Chiang et al., 1994; Welch et al., 1994). It is believed that inhibition of RNA polymerase by distamycin occurs via displacement of transcription factors from the promoter region, rather than a direct interaction with the single-stranded open complex (Mazumder et al., 1994). All of the above inhibitions entail binding to B-DNA.

Since netropsin and distamycin are cytotoxic, derivatives of these compounds have been synthesized by several laboratories seeking to improve their pharmacological properties and enhance specificity for binding to a specific DNA site (Lown, 1992; Arcamone, 1993). Promising results have been observed with bis-linked lexitropsins, or sequence-reading analogues of netropsin and distamycin (Khorlin et al., 1980; Lown et al., 1989; Kissinger et al., 1990; Rao et al., 1991; Guo et al., 1993), and lexitropsin derivatives containing alkylating agents (Krowicki et al., 1988; Arcamone et al., 1989; Montecucco et al., 1991; Broggini et al., 1995). In both of these categories of DNA-binding molecules a correlation has been demonstrated between cellular assays and DNA binding. This study focuses on the bis-linked lexitropsins.

The lexitropsin analogues of netropsin and distamycin (Figure 1) can be regarded as short polymers of amino acid-like monomers, $-NH-(P/I)-CO-$, where P/I represents a five-membered pyrrole or imidazole ring, connected by peptide linkages (Kopka et al., 1985a,b; Lown et al., 1986; Kissinger et al., 1987). Positive charges from guanidinium or amidinium groups occur at both ends of members of the netropsin family and at one end of a distamycin. A typical lexitropsin with $n-1$ pyrrole rings and n amide groups binds preferentially to minor groove sites containing $n+1$ successive A·T base pairs, a behavior that Dervan has termed the "$n+1$ rule". Oligomers of up to six $-NH-(P/I)-CO-$ units have been shown to bind to DNA in a sequence-specific manner (Youngquist & Dervan, 1985). A slight mismatch between the length of one monomer unit and the repeat
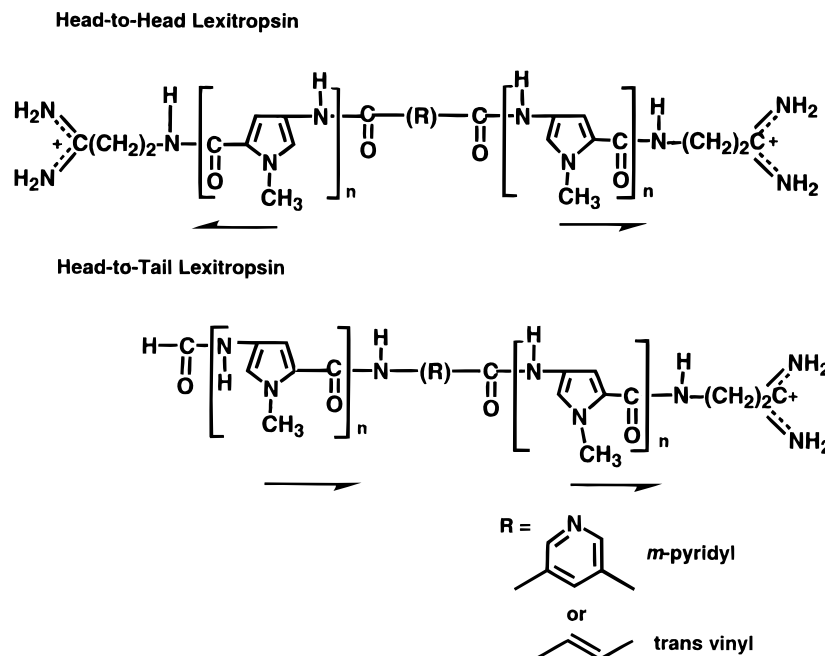
Head-to-Head Lexitropsin

Head-to-Tail Lexitropsin

FIGURE 1: Head-to-Head and head-to-tail lexitropsins. The basic monomer unit for lexitropsins is an amino acid analogue: $-NH-(P/I)-CO-$, where P/I represents a 5-membered pyrrole or imidazole ring. As with normal amino acids, the "forward" or positive chain direction is from NH to P/I to CO. Two such monomers are linked in netropsin ($n = 2$), and three in distamycin ($n = 3$). Both netropsin and distamycin end with a propylamidinium cation (shown at both right and left in the head-to-head complex). Netropsin commences with a guanidinium cation, whereas distamycin has an uncharged $H-CO-$ headgroup (shown at left in the head-to-tail complex). Linker groups are symbolized by $-(R)-$. Above: Head-to-head linkage of two netropsins or distamycins. Below: Head-to-tail linkage of two distamycins, retaining one initial $H-CO-$. Chain directions are indicated by arrows. The two best linkers from this study have been 3,5-*meta*-pyridyl or *trans*-vinyl, as shown at bottom.

between base pairs along the floor of the minor groove of B-DNA means that longer lexitropsins go "out of phase" with the DNA and bind less well (Goodsell & Dickerson, 1986). To resolve this phasing problem, pairs of shorter lexitropsins have been connected by linkers of various lengths, of such dimensions that each of the connected lexitropsin groups can remain in register with its own region of DNA (Lown et al., 1989; Walker et al., 1995). The ultimate goal, of course, is to design longer drug analogues capable of recognizing and binding specifically to a long region of defined target sequence *in vivo*.

Lown and co-workers (1989) have found a correlation between the DNA binding of methylene-linked oligopeptides derived from netropsin and distamycin, and inhibition of tumor cell proliferation in both human and murine tumor cell lines. In all of the cell lines observed, at least one of the linked drugs exhibits a greater inhibitory effect than either distamycin or netropsin. The same DNA-binding correlation also extends to antiviral activity in host cell culture for four species of virus: herpes simplex 1 and 2, vaccinia, and vesicular stomatitis (Lown et al., 1989). Minimal inhibitory concentrations for all of the linked compounds are less than minimal cytotoxic concentrations. A correlation also has been found between DNA-binding and *in vitro* inhibition of the combined RNA- and DNA-directed polymerization of MuLV associated reverse transcriptase. DNA affinity and biological activity depend on the precise positioning of the two halves of a bis-linked drug relative to their local DNA-binding sites, and this in turn depends on the length of the linker. Maximal DNA binding and inhibition are seen with linkers consisting of 1–2 or 6–8 $-CH_2-$ methylene groups. Footprinting data of Kissinger et al. (1990) have shown that the length of the linker is important in determining whether

both ends (bidentate binding) or only one end (monodentate) of the bis-linked drug will bind to DNA.

The introduction of rigid linkers instead of flexible methylene chains adds a new geometrical constraint to drug binding (Kissinger et al., 1990; Rao et al., 1991). DNA footprinting experiments reveal a preference for *trans* over *cis* rigid-linked isomers. Bidentate binding is more common with *trans* linkers; *cis* linkers tend to allow only one end of the linked drug to interact with DNA. Aryl linkers have reduced DNA binding compared to the best of the flexible linkers and the *trans* isomers (Kissinger et al., 1990).

In general, bis-linked compounds with rigid linkers tend to have greater antiviral activity than those with flexible linkers (Wang & Lown, 1992), but the correlation between DNA binding and antiviral effect is weak for retroviruses. *cis*-Vinyl netropsin, a less efficient DNA binder, proved to be the most potent rigid-linked lexitropsin for HIV in host cell culture, but *trans*-vinyl distamycin was best for MuLV.

In all of the model systems studied to date, whether *in vitro* enzyme inhibition, tumor cell cytotoxic effect, or antiviral activity in host cells, inhibition has been based on drug design studies involving the DNA duplex. But in retroviral systems the primer is RNA, as is the template itself for (−)-strand synthesis. Hence the precise conformation of RNA/RNA and RNA/DNA duplexes of different base sequences becomes critical. Past studies of groove-binding drugs in retroviral models have either not focused on transcriptional steps *per se* (Fesen et al., 1993; Subra et al., 1993; Carteau et al., 1994; Feriotto et al., 1994) or have not differentiated between RNA- and DNA-template-directed polymerization events (De Clerq & Dann, 1980; Lown et al., 1989; Wang & Lown, 1992; Ji et al., 1994). We propose that linked lexitropsins, particularly rigid-linked compounds,

offer unique ligand geometries that enhance affinity for an RT-associated RNA/DNA hybrid. For this reason we have focused on the RNA-directed DNA polymerization of HIV-1 reverse transcriptase.

MATERIALS AND METHODS

Drugs. The bisnetropsin and bisdistamycin compounds were synthesized and provided by J. W. Lown of the University of Alberta (Wang & Lown, 1992; Guo et al., 1993). Distamycin A and berenil (diminazene aceturate) were purchased from Sigma and CalBiochem, respectively. DAPI (4′,6-diamidino-2-phenylindole dihydrochloride) and netropsin were purchased from Boehringer-Mannheim. Fluka BioChemika was the source of Hoechst 33258 (bisbenzimide) and AZT (azidothymidine). Triphosphorylation of AZT was performed by Sierra Bioresearch.

Templates, Primers, and Nucleotides. Poly(rA)$_{630}$, poly-(dA)$_{270}$, poly(dI·dC), and dTTP were purchased from Pharmacia, and oligo dT$_{14}$ was obtained from Sigma and Pharmacia. The radionucleotide, [*methyl*-^{3}H]dTTP, came from Dupont NEN. Oligos (rA)$_{14}$ and (dA)$_{14}$ were purchased from Promega. Poly[U,G] RNA was purchased from Sigma. [^{32}P]GMP-labeled oligo rG$_3$A$_{20}$UGAC and [^{32}P]TMP-labeled oligo dT$_{14}$ were provided by David Sigman of UCLA. Stock solutions of drugs were prepared at 5 mM concentration in water or DMSO and stored at −80 °C.

Enzymes. Recombinant p66/p51 HIV-1 RT (Hizi et al., 1988; Clark et al., 1990) was provided by Steve Hughes of NCI. Human DNA polymerase β was purchased from Molecular Biology Resources Inc.

Enzymatic Assays. HIV-1 RT RNA-dependent DNA polymerase activity was assayed by measuring the amount of poly(rA)$_{630}$·oligo(dT)$_{14}$-directed incorporation of [^{3}H]-dTMP into acid-precipitable extended DNA product. Final reaction volume was 150 μL in RT Assay Buffer, which contained 25 mM Hepes, 75 mM KCl, 8 mM MgCl$_2$, 0.1% Triton X-100, and 2 mM DTT at pH 8.0. Final enzyme concentration was 6.0 μg/mL, as measured by Bio-Rad protein dye assay against a BSA standard. Incorporated [^{32}P]-dTMP was measured from a 50 μL aliquot quenched in 150 μL of 0.3 mg of salmon testes DNA/mL in 0.2 M NaPP$_i$, precipitated with 10% TCA, and filtered onto Whatman GF/C fiberglass filters. Filters were washed with 10% TCA and ethanol and read in a Packard 1500 Tri-Carb scintillation counter.

DNA polymerase β activity was assayed by measuring the amount of poly(dA)$_{270}$·oligo(dT)$_{14}$-directed incorporation of [^{3}H]dTMP into acid-precipitable extended DNA product. Final reaction volume was 115 μL in DNA Pol β Assay Buffer which contained 50 mM Tris, 100 mM NaCl, 1 mM MnCl$_2$, and 3 mM DTT at pH of 7.5. Final enzyme concentration was 6.0 units/mL where 1 unit is the amount of enzyme required to incorporate 1 nmol of total nucleotide into acid-insoluble form in 60 min at 37 °C. Incorporated [^{3}H]dTMP was isolated and measured as in RT assays.

RT IC$_{50}$ Drug Screens

(a) ETP Initiation. RT Assay Buffer, including drug and radiolabeled nucleotide, was pre-incubated at 30 °C for 10 min prior to addition of ETP. Reactions were initiated with a 20× concentration of enzyme−template−primer, ETP, pre-incubated at 4 °C for 3 min in RT Assay Buffer without

MgCl$_2$. Incorporation of [^{3}H]dTMP was measured after 5 min of incubation at 30 °C. Reaction rates were linear throughout the 5 min assay. Assays were performed under V_{max} conditions with regard to template concentration (poly-(rA)$_{630}$ at 5.0 μM), 0.75V_{max} with regard to primer (oligo-(dT)$_{14}$ at 50 nM), and V_{max} with regard to nucleotide (dTTP at 100 μM). The nucleotide specific activity was 0.4 Ci/mmol. Data from drug screening of MPyr and TVin were used in deriving the Dixon and Hill plots of Figure 4. Approximate IC$_{50}$ values in Table 1 (indicated by "ca." or ">") were interpolated from partial curves at 50, 100, and 200 μM concentration of drug.

(b) E Initiation. Reactions were performed as in *a* above except that TP is pre-incubated with nucleotide and drug in RT Assay Buffer (30 °C for 10 min). Reactions were initiated with an aliquot of 20× concentration of enzyme pre-incubated at 4 °C for 3 min in RT Assay Buffer without MgCl$_2$.

DNA Pol β Drug Screens

(a) ETP Initiation. DNA Pol β Assay Buffer, including nucleotide and drug, was pre-incubated at 37 °C for 10 min prior to addition of ETP. Reactions were initiated as for RT assays with ETP pre-incubated at 4 °C for 5 min in DNA Pol β Assay Buffer. Incorporation of [^{3}H]dTMP was measured after a 10 min incubation at 37 °C. Reaction rates were linear over the 10 min assay period. Assays were performed under V_{max} conditions with regard to template concentration (poly(dA)$_{270}$ at 0.2 μM), 0.75V_{max} with regard to primer (oligo dT$_{14}$ at 0.3 μM), and V_{max} with regard to nucleotide (dTTP at 120 μM). The nucleotide specific activity was 0.5 Ci/mmol.

(b) E Initiation. Reactions were performed as for RT assays except that the enzyme was pre-incubated for 5 min.

RT Challenge Assays. Assays were performed as in section *a* of RT IC$_{50}$ Drug Screens except that the final concentration of poly(rA)$_{630}$ is 0.5 μM, and RT Assay Buffer also contained 2 mg of poly[U,G] competitor RNA/mL. An aliquot of either drug or water (control) was added to the reaction mixture 1 min after reaction start, and reaction was terminated 4 min later. For the control assay 100% activity is represented as the incorporation of dTMP between 1 and 5 min after reaction start, and IC$_{50}$ values are calculated accordingly.

ΔT_m Analysis—rA$_{14}$·dT$_{14}$ and dA$_{14}$·dT$_{14}$. 0.4 OD units of oligomers in 1:1 ratio were annealed in 0.5 M NaCl by heating to 90 °C and cooling slowly to room temperature overnight. Drug was added at a final drug:oligomer ratio of 2.5:1, and the sample was cooled to 8 °C. Absorbance (260 nm) vs temperature profiles were measured over a range of 8−56 °C on a Beckman DU65 spectrophotometer, using a Peltier block for temperature control. The temperature was increased linearly at 2 °C/min, and ΔT_m was determined from a derivative plot of absorbance vs temperature.

Steady State Kinetics. Initial linear enzyme velocities were determined from assays performed as in section *a* of RT IC$_{50}$ Drug Screens. When nucleotide (dTTP) is the variable substrate, nucleotide concentrations are 18.2, 23.5, 33.3, 57.1, and 133 μM, with template (poly(rA)$_{630}$) at 0.5 μM concentration and primer (oligo(dT)$_{14}$) at 200 nM. When primer is the variable substrate, primer concentrations are 18.2, 22.2, 28.6, 40, 66.7, 100, and 200 nM with template (poly(rA)$_{630}$)

Table 1: Comparison between Antiviral Activity and *in Vitro* RT Inhibition[a]

linked drug	linker	linkage type	linkage geometry	RT IC$_{50}$ (μM)	viral EC$_{50}$ (μM)	TI$_{50}$
netropsin	none	monomer	none	170	—	—
Hoechst 33258	none	monomer	none	220	—	—
distamycin	none	monomer	none	250	—	—
DAPI	none	monomer	none	250	—	—
berenil	none	monomer	none	600	—	—
netropsin	($-CH_2-$)	flexible	H−T	ca. 150	—	—
	($-CH_2-$)$_2$	flexible	H−T	145	—	—
	($-CH_2-$)$_3$	flexible	H−T	>200	—	—
	($-CH_2-$)$_4$	flexible	H−T	>200	—	—
	($-CH_2-$)$_5$	flexible	H−T	ca. 180	—	—
	($-CH_2-$)$_7$	flexible	H−T	>200	—	—
	($-CH_2-$)$_7$	flexible	H−H	>200	2.1	24.1
distamycin	($-CH_2-$)$_2$	flexible	H−H	360	41	1.0 (inactive)
	($-CH_2-$)$_6$	flexible	H−H	>400	—	inactive
	($-CH_2-$)$_8$	flexible	H−H	>500	14	2
	($-CH_2-$)$_{22}$	flexible	H−H	>500	—	inactive
Im$_2$-lexitropsin	*trans*-vinyl	rigid	H−H	ca. 150	—	—
netropsin	*m*-phenyl	rigid	H−T	ca. 150	—	—
	m-phenyl	rigid	H−H	ca. 150	3.55	80
	cis-vinyl	rigid	H−H	200	0.35	566
	trans-vinyl	rigid	H−H	ca. 200	1.37	24.1
	p-phenyl	rigid	H−T	>300	1.21	14.8
distamycin	**3,5-*m*-pyridyl**	**rigid**	**H−H**	**28**	**9.8**	**7**
	2,6-*m*-pyridyl	**rigid**	**H−H**	**70**	**13**	**11**
	***trans*-vinyl**	**rigid**	**H−H**	**68**	**10.4**	**19.8**
	***cis*-vinyl**	**rigid**	**H−H**	**90**	**—**	**inactive**
distamycin	*m*-phenyl	rigid	H−H	ca. 150	21	6.6
	1,3,5-phenyl	rigid	H−H	ca. 150	—	—
	o-phenyl	rigid	H−H	>300	—	—
	2,5-*p*-pyridyl	rigid	H−H	>500	1.6	43
	trans-1,2-cyclobutyl	rigid	H−H	>800	16	4.5
	5,6-(2-norbornenyl)	rigid	H−H	>900	—	—

[a] H−H, head-to-head drug molecule linkage; H−T, head-to-tail linkage; Im$_2$, di-imidazole; IC$_{50}$ (RT) from this work; EC$_{50}$ (viral) and TI$_{50}$ from Wang and Lown (1992).

at 0.5 μM and nucleotide (dTTP) at 100 μM. Double-reciprocal plots were obtained from computer-aided linear regression fits (r^2) of calculated enzyme rates (Macintosh Cricket software). In a similar manner, K_i determinations were made from computer-aided linear regression fits of slope and intercept data obtained from double-reciprocal plots.

PAGE Mobility Shift Assays. RT−template−primer complex was characterized by electrophoretic retardation of a [^{32}P]-radiolabeled RNA/DNA hybrid, rG$_3$A$_{20}$UGAC/dT$_{14}$, after incubating first with enzyme and then with drug. RT−template−primer complex was incubated at 4 °C for 20 min in 10 mM HEPES-NaOH, pH 8.0, 50 mM NH$_4$SO$_4$, 0.25 mM DTT, 0.7 mg of poly(dI)·poly(dC) competitor DNA/mL, and 10% glycerol. A 15× aliquot of drug was added, and the mix was incubated an additional 15 min. The 15 μL gel load contained 0.60 pmol of [^{32}P]GMP-labeled RNA, 0.12 pmol of [^{32}P]dTMP-labeled DNA, and 2.4 pmol of HIV-1 RT. Protein−oligo mixtures, with or without drug, were electrophoresed through an 8% polyacrylamide gel containing 2% glycerol with 0.5× TBE buffer at 4 °C under 12 V/cm for approximately 2 h. Gels were then dried and autoradiographed.

RESULTS

IC$_{50}$ Screening of Monomeric and Bis-Linked Drugs

Twenty-nine linked lexitropsins, some previously evaluated for anti-HIV-1 activity in host cells (Wang & Lown, 1992), and five classic groove-binding drugs were screened for their inhibitory effect against HIV-1 RT RNA-dependent polymerization as shown in Table 1. The drugs are listed in categories corresponding to type of linkage, flexible or rigid, and type of drug ligand, in order of increasing RT IC$_{50}$ for each category. Ligands of the type shown in Figure 1 are either di- or tripyrroleamides related to netropsin and distamycin, linked in head-to-tail (H−T) or head-to-head orientation (H−H). Antiviral EC$_{50}$ and TI$_{50}$ indices of Wang and Lown (1992) are included in Table 1 where available. TI$_{50}$ is defined as the ratio of IC$_{50}$ for cellular toxicity in uninfected cells to the viral EC$_{50}$, which measures protection in infected cells (Weislow et al., 1989). Hence TI$_{50}$ values are a gauge of antiviral selectivity; the larger the value, the more selective the drug for virus over host.

Classic groove-binding monomers, in general, exhibit poor or moderate inhibition at best (Figure 2). It is interesting to note that netropsin is a better inhibitor than distamycin, with IC$_{50}$ of 170 vs 250 μM. Distamycin with its three pyrrole rings and four amides binds to five consecutive A·T base pairs, while netropsin with its two pyrroles and three amides binds only to four A·T pairs (Patel, 1982; Van Dyke & Dervan, 1983; Kopka et al., 1985a,b). More significantly, distamycin has a single cationic end whereas netropsin has two. For these two drug monomers, cationic charge seems to play a more important role in binding than does the number of base pairs in the binding site.

The situation is blurred somewhat in the linked lexitropsins (Figure 1). H−H- and H−T-linked netropsins and H−H-
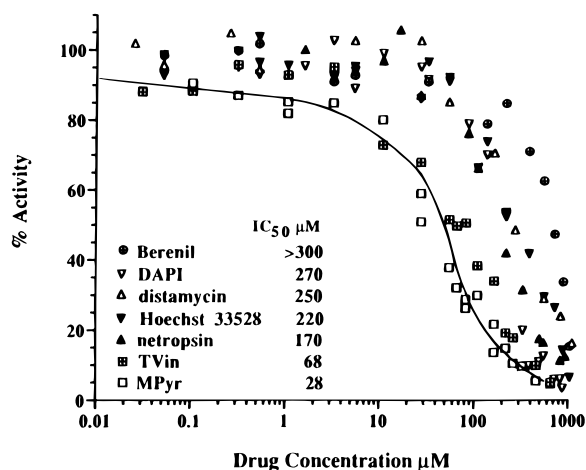
FIGURE 2: Activity curves and IC$_{50}$ values for inhibition of HIV-1 reverse transcriptase RNA-directed DNA polymerization by groove-binding drugs. Classic monomeric groove-binding drugs exhibit either comparatively moderate inhibition with IC$_{50}$ s in the range 100−300 μM (DAPI, distamycin, Hoechst, netropsin) or poor inhibition with IC$_{50}$ values over 300 μM (berenil). The best two bis-linked inhibitors were *trans*-vinyl (TVin) and 3,5-*meta*-pyridyl (MPyr) head-to-head bis-distamycins, with IC$_{50}$ values of 68 and 28 μM, respectively. A smooth curve is shown only for MPyr.
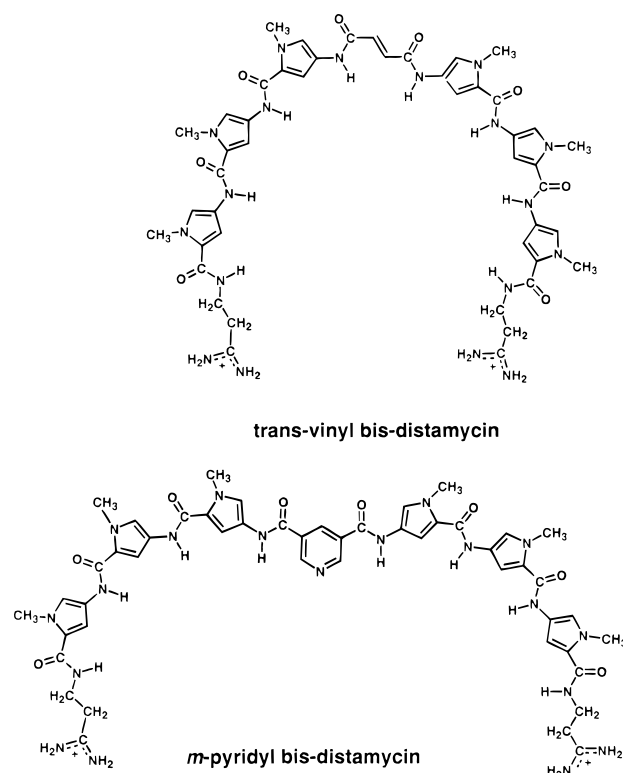

FIGURE 3: Molecular structures of TVin (top) and MPyr (bottom). TVin and MPyr consist of two bis-linked distamycins with a vinyl and a pyridine linker, respectively. The distamycin moieties consist of a propylamidinium tail followed by an amide and a pyrrole ring repeated three times, plus a final amide before the linker.

linked distamycins all have a positive charge at each end and differ principally in the greater length of the distamycin derivatives. H−T-linked distamycins, in contrast, have only a single positive charge. IC$_{50}$ comparisons of H−T vs H−H linkages of netropsin (Table 1) reveal little difference when the linker is the same, with (−CH$_2$−)$_7$ or *m*-phenyl for example, but this is only to be expected since both the overall length and overall charge on the bis-linked drug are unaltered. No H−T-linked distamycins were included in the study, so the charge issue *per se* is not addressed. When length is varied keeping charge constant, as with equivalently linked H−H distamycins and H−H netropsins, the longer distamycins clearly are the better inhibitors *in vitro*. (Compare *cis*- and *trans*-vinyl linkers.)

Linked-lexitropsin inhibitors of RT *in vitro* can be categorized for convenience in three IC$_{50}$ ranges: effective, with IC$_{50}$ values below 100 μM; mid-range, with IC$_{50}$ values from 100 to 300 μM; and ineffective, with IC$_{50}$ values greater than 300 μM. The effective inhibitors, highlighted in Table 1, are all rigid-linked bis-distamycins with either *meta*-pyridyl or vinyl linkers. Mid-range inhibitors include distamycins with rigid *meta*-phenyl linkers and virtually all bis-netropsins, whether their connections are rigid or flexible. Inhibitors using rigid aryl linkers with other than *meta* linkages are generally ineffective, as are flexibly linked distamycins.

Nearly all of the rigidly-linked drugs for which viral EC$_{50}$ and TI$_{50}$ values were determined by Wang and Lown (1992) show antiviral selectivity (TI$_{50}$ > 6), yet only four are effective RT inhibitors *in vitro* (IC$_{50}$ < 100). Indeed, one of these four, *cis*-vinyl distamycin, is inactive in the viral assay (Weislow et al., 1989; Wang & Lown, 1992). *cis*-Vinyl netropsin is by far the most potent inhibitor in the viral EC$_{50}$ cell culture assay, but not in the RT IC$_{50}$ *in vitro* assay.[1] Flexible linked bis-distamycin drugs used in both

assays are poor inhibitors against RT, and their effectiveness decreases with the length of the methylene linker (IC$_{50}$ = 360 to >500). In contrast, antiviral EC$_{50}$ values for these drugs do not appear to exhibit this methylene linker-dependent trend and the drugs are largely non-selective (TI$_{50}$ < 2 or "inactive"). All of these comparisons suggest that RNA-directed polymerization by reverse transcriptase may not be the specific target of the drug in viral cell culture assays and that the IC$_{50}$ and EC$_{50}$ columns in Table 1 may be measuring different inhibitory activities.

Figure 2 shows activity vs concentration behavior for several of the most relevant drugs. The two best inhibitors from IC$_{50}$ determinations are 3,5-*meta*-pyridyl bisdistamycin (MPyr) and *trans*-vinyl bisdistamycin (TVin), with IC$_{50}$ values of 28 and 68 μM, respectively. Their structures are shown in Figure 3. The linear Dixon plots for MPyr and Dst (distamycin) in Figure 4A indicate a single binding site, whereas the parabolic curve for TVin suggests multiple-site binding. This behavior is reiterated in the Hill plot of Figure 4B, which indicates a single inhibitor binding site for MPyr and two sites for TVin.

Inhibition: Processive Addition vs TP Turnover Steps

RNA-directed DNA polymerization by HIV-1 reverse transcriptase *in vitro* has been shown by Majumdar et al. (1988) to follow an ordered bireactant−biproduct (Bi−Bi) mechanism, in which template−primer (TP) binds prior to nucleotide (N), and the cleaved nucleotide pyrophosphate (PP$_i$) falls away while elongated TP still is bound to enzyme. Rittinger et al. (1995) have proposed two conformation changes in the enzyme; one after binding TP and the second

---

[1] *cis*-Vinyl netropsin was found to inhibit *in vitro* strand transfer and disintegration reactions mediated by HIV-1 integrase with an IC$_{50}$ of approximately 25 μM (S. Chow, personal communication).
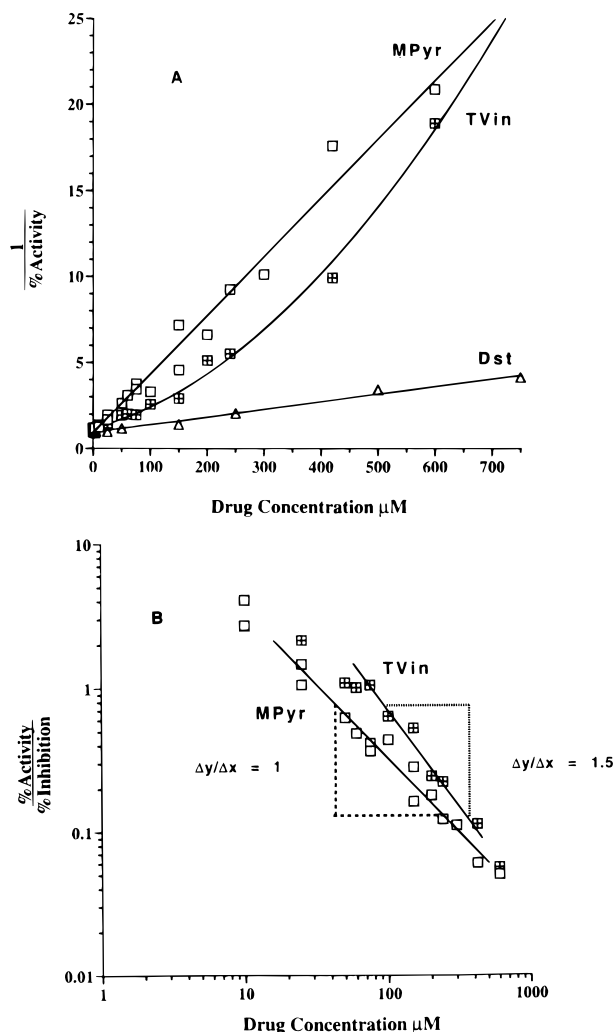
FIGURE 4: Characterization of distamycin, MPyr, and TVin interaction at the enzyme active site. (A) Dixon plots of distamycin (Dst) and its head-to-head bis-linked derivatives with linkers *trans*-vinyl (TVin) and *meta*-pyridyl (MPyr), normalized at 100% activity = 1. MPyr and Dst plots are linear, indicating a single drug-binding site. TVin, with a parabolic plot, has more than one drug-binding site. (B) Hill plots for MPyr (open squares) and TVin (crossed squares). The MPyr plot is linear with unit slope throughout the activity/inhibition range. In contrast, the TVin plot is curved, with a slope approaching 1.0 at low drug concentrations (left), 2.0 at high concentrations, and an intermediate slope of ca. 1.5, again suggesting two-site drug binding (Segel 1975).

after binding N. Consideration of this and other work leads to the mechanism diagrammed in Figure 5. The cycle involving processive addition of nucleotides to the primer chain is shown at right, and the entry and exit to the cycle during turnover steps is at left.

Reverse transcriptase normally adds a certain number of mononucleotides to its growing primer strand (the processive phase) and then disassociates from the template−primer to associate immediately with the same or a different template−primer duplex (turnover) and continue polymerization. To find out what step in this process was being inhibited by the bis-linked lexitropsins, we followed the procedure of Huber et al. (1989). In this analysis, the reaction is initiated with the preformed ETP complex in the presence of excess capture RNA in the form of poly[U,G]. As soon as an enzyme molecule disassociates from its original TP, it is immediately captured by excess poly[U,G] and eliminated from the reaction in a dead-end complex. Hence the only enzyme

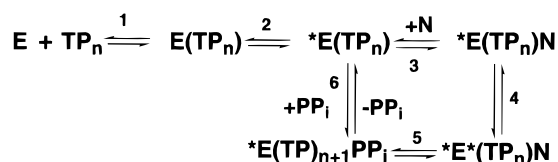**Entry and Exit to Processive Cycle   Processive Cycle**

FIGURE 5: Ordered bireactant−biproduct (Bi−Bi) mechanism for DNA polymerization by HIV-1 RT as established by Majumdar et al. (1988) and Rittinger (1995). Free enzyme, E, binds first to the template−primer, poly(rA)·oligo(dT) or TP_n (step 1), forming an enzyme−template−primer initiation complex, $E(TP_n)$. Equilibrium strongly favors $E(TP_n)$ over E and TP_n. The initiation complex then enters the processive nucleotide addition cycle. According to Rittinger the enzyme itself undergoes two conformational changes symbolized by *E and *E*: one following binding of TP_n (step 2), the other after binding of nucleotide (steps 3 and 4). The primer chain is lengthened by one base in step 5, and pyrophosphate falls away in step 6 to yield a longer $*E(TP_{n+1})$ complex, ready for another processive cycle. When the enzyme pauses and dissociates during a turnover, steps 2 and 1 are reversed.

Table 2: 50% Inhibition of HIV-1 RT in the Presence and Absence of Poly [U,G] Challenge RNA

	IC_{50} (in μM)	
drug	unchallenged (multicycle)	challenged (single cycle)
distamycin	250	850
TVin	68	425
MPyr	28	630

available for drug inhibition is that which is still bound to its original TP, and only the processive phase of RT activity is studied.

In this manner Dst, TVin, and MPyr were assayed for their ability to inhibit single processive polymerization. Drug was added to the reaction mixture after initiation with the ETP complex. IC_{50} values were measured and compared with those obtained under conditions in which more than one processive cycle was allowed. The results are shown in Table 2. All three drugs are markedly less effective as inhibitors when confined only to the processive phase of synthesis. Dst is worse by a factor of 3.4, TVin by a factor of 6.2, and MPyr by a factor of 22.5. This indicates that the primary moment of inhibition by these drugs, especially MPyr, is not during processive polymerization, but rather at initiation or termination steps between processive cycles—at steps 1 or 2 in Figure 5.

Inhibition upon Incubation of Drug with TP vs ETP: HIV RT

In order to pinpoint the locus of inhibition more closely, parallel experiments were carried out in which (a) the drug in question was first incubated with TP prior to addition of enzyme or (b) enzyme and TP were pre-incubated prior to addition of drug. The order of addition of reactants is completely immaterial for distamycin. The same $IC_{50} = 250$ μM results no matter whether the experimental protocol is E + TPI → products or ETP + I → products, where I is the inhibitory drug. The behavior of TVin is very similar, with perhaps some small measure of enhancement under ETP initiation conditions, as reflected in a moderately reduced IC_{50} value, from 95 to 68 μM. However, with MPyr (Figure 6), surprisingly an almost 4-fold increase in inhibition occurs
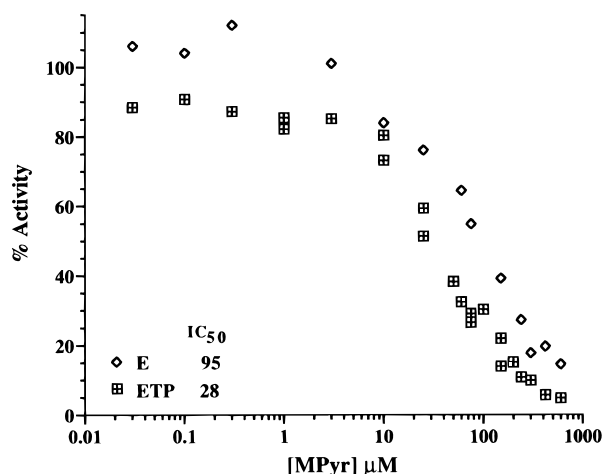
FIGURE 6: Effect of order of reagent addition on MPyr inhibition of HIV RT RNA-dependent DNA polymerization. Open diamonds, E initiation: reaction is started by addition of enzyme (see Materials Methods). Crossed squares, ETP initiation: reaction is started with enzyme pre-incubated with template−primer. Final concentrations of all reagents are identical for E and ETP initiation. IC$_{50}$ values in μM are shown for each experiment. In comparison to distamycin and TVin the order of addition of reagents is quite important for MPyr, with a preference for pre-incubation of TP with E (see Table 3).

when the reaction is initiated with ETP, the IC$_{50}$ dropping from 95 to 28 μM.

These results are summarized in Table 3. For MPyr the enzyme−template−primer complex apparently is a significantly better drug-binding site than is free template−primer. The simplest interpretation is that prior binding of TP to the enzyme surface induces a helix conformation in TP that is more receptive to the drug. PAGE gel electrophoresis experiments below demonstrate that MPyr does bind to some extent to free TP, and in fact induces formation of TP from separate template and primer strands. But the enzyme may assist the drug even further by optimizing the helix conformation for interaction with MPyr.

Inhibition upon Incubation of Drug with TP vs ETP: Human Polymerase β

As a control, the experiments of the last section with HIV reverse transcriptase were repeated with human DNA polymerase β to assay any difference in behavior of the three inhibitors with a different polymerase. Distamycin and bis-linked lexitropsins have been shown to be effective binders of B-DNA (Zimmer et al., 1971a; Wartell et al., 1974; Kissinger et al., 1990; Rao et al., 1991), and the inhibitory effect of distamycin in DNA polymerase assays employing a duplex DNA template−primer has been demonstrated (Puschendorf & Grunicke, 1969; Zimmer et al., 1971b; Wahnert et al., 1975). However, no systematic comparisons have been made of inhibition by these lexitropsin drugs of RNA- vs DNA-directed DNA synthesis.

As described under Materials and Methods, an *in vitro* assay of human DNA polymerase β inhibition used poly-(dA)$_{270}$·oligo(dT)$_{14}$ as its template−primer complex rather than the poly(rA)$_{630}$·oligo(dT)$_{14}$ used as template−primer in the HIV-RT assays just described. Experimental conditions were chosen to parallel those in the RT inhibition assay. IC$_{50}$ values for both RT and Pol β are compared in Table 3. All three drugs inhibit Pol β better than RT, as indicated by lower

IC$_{50}$ values, but Pol β consistently prefers E initiation, or pre-incubation of drug with free TP rather than with ETP, the reverse of the behavior of MPyr with RT. Of the three drugs tested, MPyr shows the most extreme variation in properties: the greatest preference for ETP over free TP with RT (3.4-fold difference in IC$_{50}$, Figure 6) and the greatest preference for TP over ETP with Pol β (10-fold difference in IC$_{50}$, Figure 7).

The consistent preference of these inhibitors for Pol β over RT suggests that they prefer to bind to a B-form dA·dT rather than a presumably more A-like rA·dT hybrid. This is only to be expected, from the known binding preferences of distamycin and netropsin. With Pol β, where the free DNA TP complex is certainly in the B-form, prior binding of TP to the enzyme apparently is an impediment to interactions with these drugs. By contrast, the free TP complex of RT is an RNA/DNA hybrid. To the extent that this hybrid approximates an A-helix, it should be a poor substrate for binding inhibitors of the distamycin/netropsin/lexitropsin family. Such drugs are known to bind within the narrow minor groove of B-DNA, and that groove is opened up and flattened out in the A-form. But netropsin and distamycin are themselves capable of inducing an A-to-B helix transition in solution (Luck & Zimmer, 1973; Zimmer, 1975), presumably by binding only to the B-form, thus shifting the A $\rightleftharpoons$ B equilibrium to the right. If indeed binding of MPyr to a free RNA/DNA hybrid duplex is mandatorily associated with an A-to-B helix transition, this could exact a cost in free energy that is not required by simple passive binding to a preformed B-helix. Favored interaction of MPyr with ETP then may result because binding of TP to the enzyme surface induces a more B-like conformation at the drug-binding locus.

Relative Binding to Free TP: Duplex ΔT_m Analysis

The relative binding affinities of MPyr, TVin, and Dst for free template−primer (not the ETP complex) can be assayed by observing the rise in duplex melting temperature produced by drug binding to (rA)$_{14}$·(dT)$_{14}$, the analogue of RT template−primer, and (dA)$_{14}$·(dT)$_{14}$, the analogue of Pol β template−primer. Results are shown at the right of Table 3. As expected, efficient inhibition of Pol β with its DNA/DNA template−primer by all three drugs (IC$_{50}$ = 0.8−1.0 μM) is matched by tight binding of those same drugs to the DNA (ΔT_m = 36−40 °C). All three drugs have larger ΔT_m values and bind better to the DNA duplex than to the RNA/DNA hybrid. This is only to be expected from the known preference of netropsin and distamycin for a B helix. With a DNA/DNA duplex there is little difference in ΔT_m from one drug to another, consistent with the finding that E initiation with Pol β is essentially the same for all three drugs.

But Table 3 reinforces the proposal that the RNA/DNA template−primer is not the optimal site of inhibition of reverse transcriptase. Binding of all three drugs to the RNA/DNA hybrid is substantially worse than to DNA/DNA, with ΔT_m of only 4−10 °C. And distamycin, the drug that binds best to RNA/DNA by the melting point criterion, is the least effective inhibitor of RT among the three. As already suggested by the E vs ETP comparisons, passive drug binding to free RNA/DNA template−primer apparently is not the most efficient road to inhibition of reverse tran-

Table 3: Comparison for RT vs DNA Pol β Inhibition with ΔT_m Measurements for Hybrid and B-DNA Oligomers

| | inhibition IC_{50} (μM) | | | | ΔT_m (°C) | |
| | RT | | DNA Pol β | | | |
drug	E init.	ETP init.	E init.	ETP init.	$rA_{14} \cdot dT_{14}$ ($T_m = 12$ °C)	$dA_{14} \cdot dT_{14}$ ($T_m = 22$ °C)
distamycin	250	250	1.0	4.0	10	41
TVin	95	68	0.8	2.0	6	36
MPyr	95	28	0.8	8.0	4	39
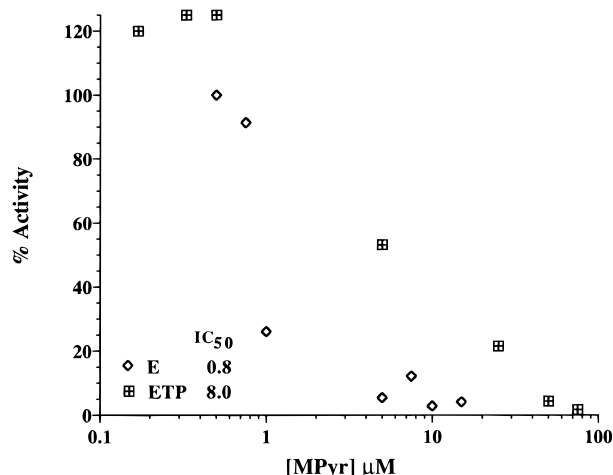
FIGURE 7: Effect of order of reagent addition on MPyr inhibition of polymerase β DNA-dependent DNA polymerization. Plot conventions as for Figure 6. IC_{50} values in μM are shown for each experiment. The order of addition of reagents is significant with the E-initiated reaction now being more effective for MPyr as well as distamycin and TVin (See Table 3).

scriptase. The bis-linked MPyr and TVin evidently want a more B-like binding site.

Kinetic Characterization of RT Inhibition by TVin

Steady state kinetics were achieved in the HIV-1 RT RNA-dependent DNA polymerization reaction by increasing the concentrations of the two substrates, primer (oligo(dT)$_{14}$) and nucleotide (dTTP), in the presence of increasing inhibitor concentrations. Kinetic characterization was limited to reactions initiated by pre-incubated ETP so that interactions of the drug with free TP are limited.

When the inhibition of a nucleoside analog or a non-nucleoside inhibitor that binds to the enzyme is studied, variations of TP concentration can be made at a constant ratio of T:P (Majumdar et al., 1988). When the inhibition is more likely occurring by interaction of the drug with the TP hybrid duplex region, it is helpful to focus on the element of TP that determines the polymerization initiation site, the primer (Majumdar et al., 1989; Sobol et al., 1991; Basu et al., 1992; Andreola et al., 1993; Delahunty et al., 1994). By varying the stoichiometry of poly(rA)$_{630}$ and oligo(dT)$_{14}$, enzyme response to each can be observed independently. By using TP in different ratios with the template concentration held constant, the enzyme response to primer is clearly defined (Nevinsky et al., 1992).

(a) Variable Primer. Double-reciprocal plots for TVin (Figure 8A) at variable primer concentrations [P] illustrate classical noncompetitive inhibition, suggesting that the enzyme primer-binding site and drug-binding site are not mutually exclusive. Slope and intercept replots in Figure 8B are overlapping hyperbolic functions of TVin concentration, indicating partial non-competitive inhibition (Segel,
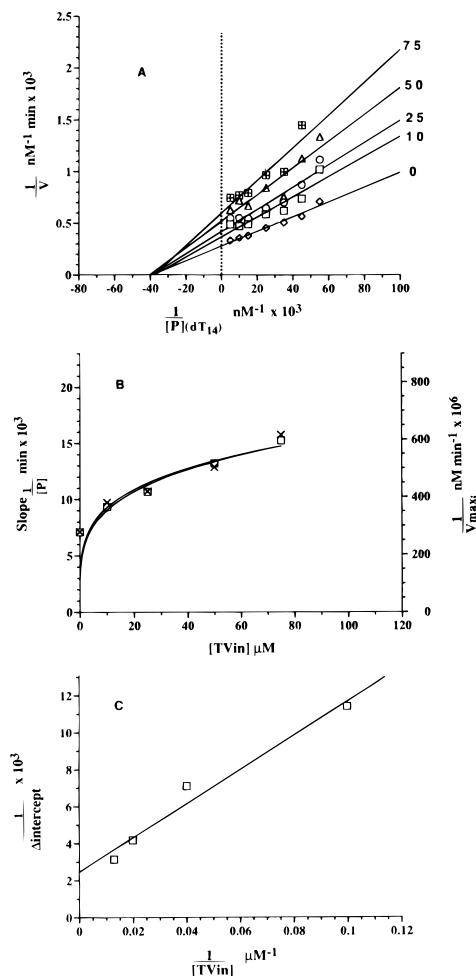

FIGURE 8: Kinetic analysis of TVin using primer (dT$_{14}$) as the variable substrate. [T] and [N*] are constant and saturating. (A) Double-reciprocal plots at TVin concentrations of 0 (control), 10, 25, 50, and 75 μM, indicating simple intersecting noncompetitive inhibition. (B) Hyperbolic slope (crosses) and intercept (squares) replots from 8A indicate partial noncompetitive inhibition. (C) Replot of reciprocal Δintercept from 8B [where Δintercept = Δ_{in} = $1/V_{max}$(drug) − $1/V_{max}$(control)] vs reciprocal inhibitor concentration, and $1/\Delta_{in} = [K_i V_{max}/(1 − \beta)](1/[TVin]) + \beta V_{max}/(1 − \beta)$. A K_i of 15.0 μM and β factor of 0.41 are determined from the slope and y-intercept of the linear regression fit: $y = 91.749x + 2.469$ with $r^2 = 0.968$. The y intercept, 2.469, is $\beta V_{max}/(1 − \beta)$, and V_{max} is 3.61 from 8A (Segel, 1975).

1975). This implies that binding of drug to either free TP or enzyme-bound TP is incomplete and that polymerization, although impeded, can proceed. The binding of drug to TP apparently does not affect the binding of enzyme to TP. A K_i value of 15.0 μM is obtained from the Δintercept replot in Figure 8C, and the partial inhibition is characterized by a turnover factor, "β", of 0.41 (Segel, 1975).

(b) Variable Nucleotide. Double-reciprocal plots for TVin (Figure 9A) with variable [N] indicate a mixed-type inhibition at the enzyme nucleotide-binding site. The lines fail to

Table 4: Kinetic Characterization of HIV-1 RT Inhibition

drug	IC_{50} (μM)	K_i (P) (μM)	K_i (N) (μM)	inhibition (P)	inhibition (N)
AZT	0.45	0.140	0.041	uncompetitive[a]	competitive[a]
MPyr	28	6.5	96	competitive	uncompetitive
TVin	68	15	94[b]	partial noncompetitive	mixed multisite

[a] From Heidenreich et al. (1990). [b] As estimated from lower linear inhibition range of intercept replot.
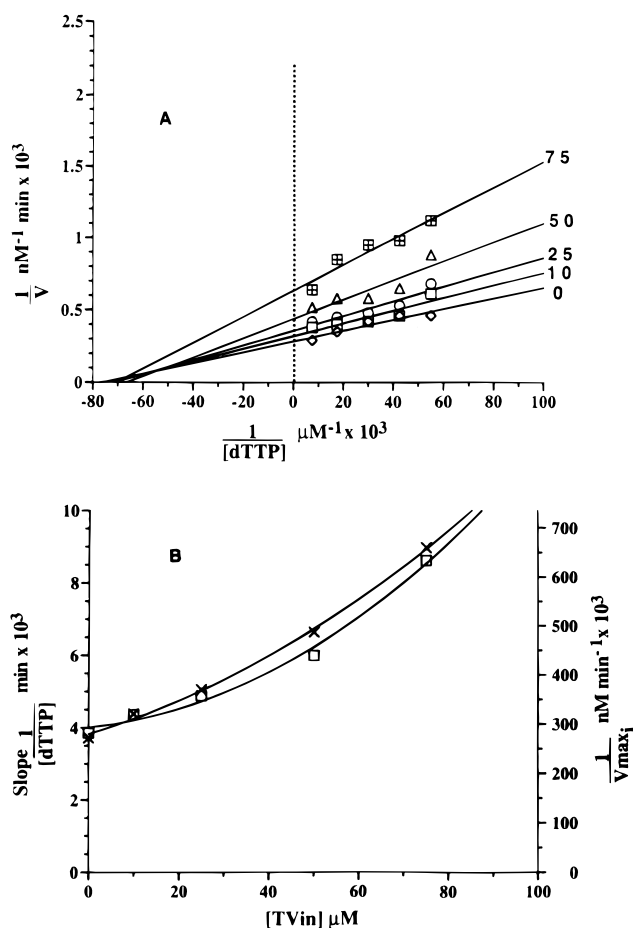

FIGURE 9: Kinetic analysis of TVin with nucleotide (dTTP) as variable substrate. [T] and [P] are constant and saturating. (A) Double-reciprocal plots at TVin concentrations of 0 (control), 10, 25, 50, and 75 μM. Non-intersection of lines on the horizontal axis indicates mixed linear inhibition. (B) Replots of slope (crosses) and intercept (squares) from 9A are parabolic and non-overlapping at higher [TVin], and linear and overlapping at lower [TVin]. An apparent K_i of 94 μM was calculated using the linear range of the intercept replot at [TVin] = 10−25 μM where the x-intercept = $-K_i$.

intersect at a common point, a result of different slope and intercept effects. Figure 9B shows that the slope and intercept replots are non-overlapping parabolic functions at higher TVin concentrations, suggesting mixed inhibition. However, at lower TVin concentrations in the range of 10−25 μM, overlapping linear replots and a common intersection point in the reciprocal plots of Figure 9A suggest a noncompetitive mode of inhibition with an apparent K_i value of 94 μM. The parabolic effect above 25 μM TVin agrees with the multiple interactions noted in the Dixon and Hill plots of Figure 4.

Kinetic Characterization of RT Inhibition by MPyr

(a) Variable Primer. The double-reciprocal plots for MPyr with variable primers concentrations [P] (Figure 10) show competitive inhibition with a common intercept equal to $1/V_{max}$. The slope replot vs MPyr concentration is a linear function of drug concentration in contrast to TVin inhibition with variable [P] (Figure 8B). This indicates complete inhibition, with drug-binding locus and enzyme active site overlapping. A K_i value of 6.2 μM for the competitive inhibition with variable [P] is determined directly from the slope replot.

(b) Variable Nucleotide. With nucleotide as the variable substrate, double-reciprocal plots in Figure 11 reveal uncompetitive inhibition for MPyr with respect to the nucleotide-binding site as demonstrated by the lack of a slope (competitive) effect. A replot of intercepts vs MPyr concentration is linear, indicating complete inhibition. The MPyr interaction is limited to reaction intermediates which are not reversibly connected to nucleotide incorporation. This agrees with dead-end competitive inhibition with variable primer. Table 4 compares the IC_{50} and K_i values for TVin, MPyr, and AZT.

PAGE Mobility Shift Assay

The inability of MPyr to inhibit the processive phase of RT polymerization shows that MPyr must act either at the initial association of enzyme with TP, or at dissociation from the extended TP, not during processive chain elongation at the working ETP site. A possible inference from this would be that inhibitor interacts with free substrate between processive cycles (TP$_n$ at left in Figure 5), rather than with enzyme−substrate complex. In contrast, the enhanced inhibition by MPyr in ETP initiation reactions and lack of correlation with melting point assays involving free TP analog suggest that the primary interaction of MPyr is with RT-bound ETP (E(TP$_n$) in Figure 5) rather than free TP. Kinetic analysis indicates dead-end inhibition with competition at drug-binding and TP-binding sites, which of itself does not discriminate between displacement of TP by inhibitor or inactivation by formation of a ternary complex.

PAGE mobility shift assays help clear up the picture. The shifts in ETP and TP bands after MPyr is added to pre-incubated E+TP are shown in Figure 12. The TP analog, radiolabeled r(G$_3$A$_{20}$UGAC)·d(T)$_{14}$, contains an internal rA$_{14}$·dT$_{14}$ homo-oligomeric duplex, with mixed-sequence 5′ and 3′ RNA template overhangs to prevent interbridging and concatenation of TP molecules.

Figure 12 shows a single PAGE gel at two different exposures, to clarify details in the top and bottom halves of the gel. Even in the absence of enzyme, MPyr promotes the association of template and primer into a TPI complex (Figure 12B, lanes 2 and 3), and eventually leads to precipitation of TPI (Figure 12A and B, lane 3). If enzyme is present but not drug, a certain small fraction of TP associates with enzyme in an ETP complex (Figure 12A, lanes 4 and 7), but addition of drug shifts the equilibria of both of the following reactions to the right

$$T + P \rightleftarrows TP \underset{-E}{\overset{+E}{\rightleftarrows}} ETP \qquad (1)$$

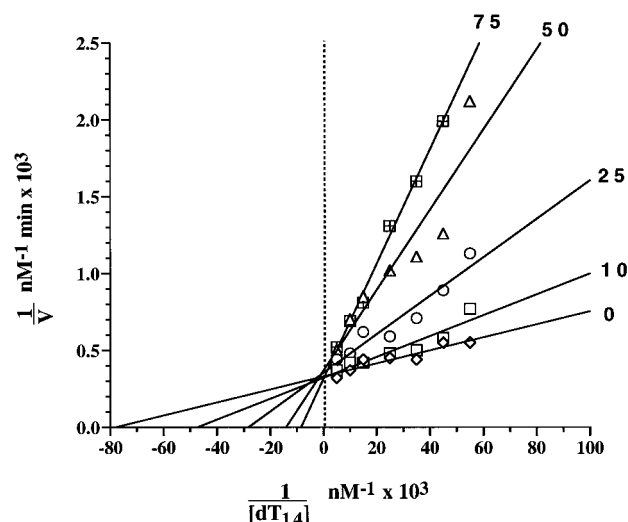increasing the intensity of both TP (Figure 12B, lanes 5 and 8) and ETP bands (Figure 12A, lanes 5 and 8).

FIGURE 10: Kinetic analysis of MPyr with primer (dT_{14}) as variable substrate. [T] and [N] are constant and saturating. Double-reciprocal plots at MPyr concentrations of 0 (control), 10, 25, 50, and 75 μM, indicating simple intersecting competitive inhibition. A linear slope replot indicates non-mixed complete inhibition with a K_i of 6.5 μM calculated from the x-intercept, $-K_i$.
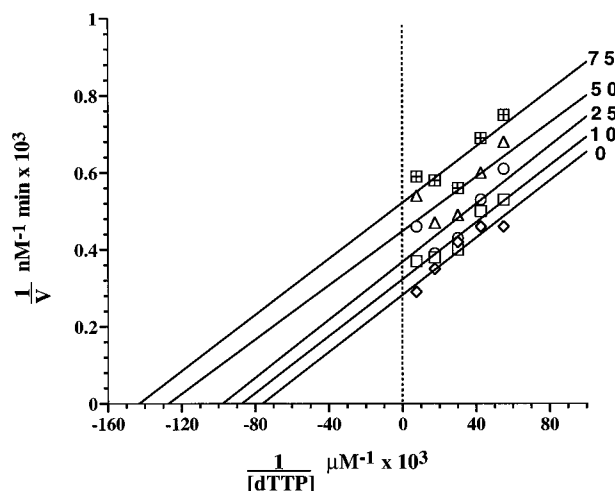

FIGURE 11: Kinetic analysis of MPyr with nucleotide (dTTP) as variable substrate. [T] and [P] are constant and saturating. Double-reciprocal plots at MPyr concentrations of 0 (control), 10, 25, 50, and 75 μM. Constancy of slope indicates simple linear uncompetitive inhibition. A linear intercept replot indicates non-mixed complete inhibition with a K_i of 96 μM calculated from the x-intercept, $-K_i$.

This PAGE gel demonstrates that, under ETP conditions and in the absence of nucleotide, the end product of inhibition by MPyr is not displacement of TP from the enzyme surface but rather entrapment of TP on the enzyme. In the former case the gel shift would have been in favor of free TP (the lower band). As TP increases below the IC_{50}, TP·I as well as ETP·I are formed. At an excess 40 μM drug concentration, which is above the IC_{50}, both TP and ETP are driven into the precipitate band at top (Figure 12A), and mass action leads to decreased intensity of the T+P band (Figure 12B).

DISCUSSION

An Enzyme-Bound Substrate–Inhibitor Complex Is the True Inhibitor for MPyr

The experiments described above are important in elucidating the nature of the inhibiting complex; taken together
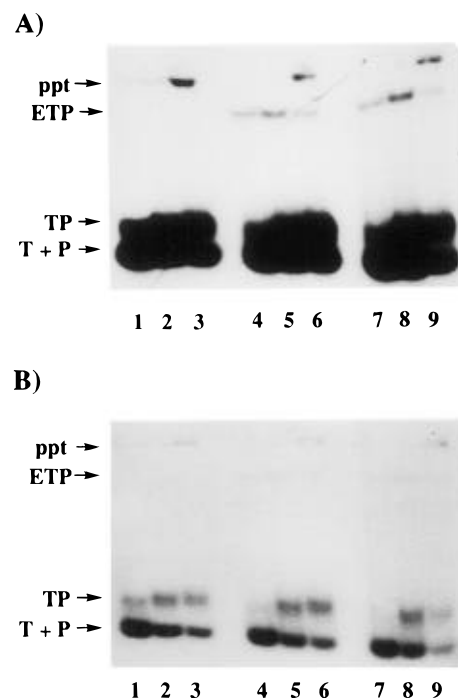

FIGURE 12: PAGE-band mobility effects of MPyr binding to ^{32}P-labeled *unannealed* template (T) plus primer (P) and T+P pre-equilibrated with RT (E). A and B are long (7.5 h) and short (4 h) exposures of the same autoradiograph. Lanes 1−3: Predominantly unannealed T+P, with MPyr (I) concentrations of 0, 20, and 40 μM respectively. Lanes 4−6: Equilibrium of T+P, TP, and enzyme-bound ETP at E:P ratio of 10:1, with MPyr concentrations of 0, 20, and 40 μM, respectively. Lanes 7−9: As lanes 4−6, but with an E:P ratio of 20:1. Adding MPyr to T+P in the absence of E induces formation of TP from T+P (lane 2). MPyr (I) concentrations greater than its 28 μM IC_{50} result in a precipitate (ppt) containing $(TPI)_n$, visible at top lane 3. With E present, a faint ETP band appears even before adding inhibitor (lane 4). MPyr inhibitor enhances the ETP band by an amount roughly proportional to the concentration of E (lanes 5 and 8). The upper bands (A) demonstrate the effects of increasing concentrations of MPyr on ETP formation, while the lower bands (B) demonstrate that MPyr (I) simultaneously induces annealing of T and P to form TPI, a substrate inhibitor, SI, complex. Taken together, A and B demonstrate the formation of a ternary complex, ETPI at moderate MPyr concentrations, and precipitation at [MPyr] greater than IC_{50}.

they give a clearer picture of MPyr inhibition and its contrast with TVin:

(1) Kinetics show single-site competitive dead-end inhibition by MPyr (Figures 4 and 10) but do not pinpoint the relevant inhibited species. In contrast, TVin shows two-site partial noncompetitive inhibition (Figures 4 and 8).

(2) Experiments with capture RNA poly r[U,G] show that inhibition by MPyr does not occur during processive synthesis steps (Table 2). This agrees with the dead-end competitive inhibition shown by the MPyr kinetics (Figure 10).

(3) IC_{50} curves using RT enzyme pre-incubated with TP (ETP-initiation) show a 4-fold increase in MPyr inhibition over E initiation, in which MPyr is allowed to incubate with free template−primer before enzyme is added (Figure 6, Table 3). This favors an enzyme-bound template−primer as the inhibited species. TVin shows only a marginal preference for ETP initiation over E initiation (Table 3). In contrast, with Pol β, both drugs clearly favor E initiation (Table 3); that is, they bind best to free TP prior to its attachment to the enzyme surface. The substrate for Pol β

is a B-DNA duplex, whereas during first-strand synthesis and in the assays of this paper, the RT substrate is a RNA/DNA hybrid of presumably more A-like character. It is possible that attachment of TP to the surface of the RT enhances MPyr binding by inducing a more B-like conformation in the hybrid duplex.

(4) Melting point analyses indicate that, in the absence of enzyme, both MPyr and TVin bind to a RNA/DNA template−primer (presumably A-like) distinctly less well than to a B-helical DNA/DNA template−primer (Table 3). This suggests again that the free TP duplex is not the natural locus of inhibition. It also suggests that any increase of B-like character produced by binding of TP to the enzyme surface would enhance drug binding, as is actually observed.

(5) The PAGE gel shift experiment with MPyr (Figure 12), run with pre-incubation of enzyme and TP, establishes the entrapment of ETP by inhibitor prior to nucleotide addition, providing that the MPyr concentration is below the IC$_{50}$ value, and confirms the existence of a TP·I complex.

In the E initiation IC$_{50}$ experiments where I and TP are allowed to pre-incubate before E is added, I intervenes before step 1 in the scheme shown in Figure 5, leading to substrate depletion by formation of TP·I and a much higher IC$_{50}$. This is shown in the PAGE gel results of Figure 12A (lane 3) where the irreversible formation of TPI and depletion of TP as precipitate occur in the absence of enzyme. Therefore, under E initiation conditions the concentration of TP is reduced prior to the introduction of E at the start of the reaction. Because of this depletion, the concentration of ETP at the start of E initiation is lower than in ETP initiation. Figure 12 (lanes 4−6 and 7−9) verify that ternary complex formation precedes depletion of TP as either TPI or ETPI precipitate. ETPI formation Figure 12 (lanes 5 and 8) is proportional to the equilibrium levels of ETP prior to the introduction of drug (lanes 4 and 7), not the equilibrium levels of TP. This suggests the enzyme-bound SI complex as the primary species of inhibition and offers an explanation for the reduction of inhibition under E initiation where ternary complex formation is most likely reduced. In sum, the role of MPyr is to lock TP onto the enzyme surface in a dead-end complex, not to displace it.

A precedent for drugs that inhibit by locking down an enzyme-bound nucleic acid substrate is offered by the quinolone antibacterials that inhibit DNA gyrase (Shen et al., 1989a,b). But in contrast to the quinolones, which are cooperative single-strand binding agents, the minor groove-binding drug MPyr binds non-cooperatively to a duplex region on the TP. The ΔT_m of TP with MPyr indicates only weak binding. Association of TP with RT enzyme must enhance drug binding, probably via a change in conformation of the nucleic acid duplex. The enzyme-bound TPI is locked in a conformation that simultaneously stabilizes ETP and impedes incorporation of nucleotide. The enzyme-induced conformational change in TP facilitates tighter binding by MPyr, resulting in a dead-end ETPI complex.

A Possible Target

The turnover event between processive cycles in the poly-(rA)·toligo(dT) assay *in vitro* is similar to enzyme dissociation/association events preceding (−)-strand transfer during viral replication. During (−)-strand transfer, DNA is transcribed from the viral template until, after pausing and

enzyme dissociation/reassociation, RT RNase H degrades the RNA template from the RNA/DNA hybrid duplex at the pause site and transfers the extended primer to a new RNA template site. Because strand transfer is unique to retroviruses and is not a mechanism used by cellular polymerases, Buiser et al. (1991) and Ghosh et al. (1995) have suggested that strand transfer during (−)-strand synthesis might be an especially promising target for drug design. As an enzyme activity preceding (−)-strand transfer, pausing serves as a *possible* target event for MPyr-type inhibition. A paused enzyme necessarily must dissociate from its TP prior to RT/RNase H processing and strand transfer. It is quite possible that inhibition by MPyr could trap this paused complex and prevent dissociation of enzyme and TP. A strand transfer assay using mixed-sequence template−primers could confirm this possibility.

Structural Implications

What could be the molecular mechanism of action of a drug inhibitor that favors interaction with a B helix and binds preferentially to the ETP complex outside the processive cycle? Arnold and co-workers (Patel et al., 1995) identify three conformational changes during polymerization by HIV-1 RT: (1) upon binding of RT to nucleic acid, (2) upon addition of dNTP but before chemical catalysis, and (3) during translocation toward the new 3′-OH primer end. Various studies focusing on step (1) have characterized the binding of RT to a DNA/DNA duplex (Divita et al., 1993; Kruhoffer et al., 1993; Rittinger et al., 1995) or to a hybrid rA·dT RNA/DNA template−primer (Beard & Wilson, 1993). In these studies, rapid diffusion-limited association of enzyme and TP is followed by slow isomerization. This ETP isomerization has been proposed recently as the rate-limiting step in single-nucleotide turnover assays on rA·dT template−primers (Jaju et al., 1995). In single-nucleotide turnover, isomerization occurs prior to nucleotide addition and then is reversed after dissociation of the elongated template−primer. These results indicate that energy-requiring conformational changes in both enzyme and nucleic acid are needed at the turnover step, apart from nucleotide incorporation. Zhan et al. (1994) also postulate a conformational change in the enzyme on binding to the hybrid duplex and state that this conformational state can be influenced by the composition and/or structure of the duplex.

In the absence of direct structural data on an RT-bound RNA/DNA hybrid duplex, two different structures have been proposed for the bound duplex: (1) a pure A-helix conformation (Kohlstaedt et al., 1992; Metzger et al., 1993) or (2) the intermediate heteromerous conformation originally proposed in the fiber diffraction experiments on poly rA·oligo dT of Arnott et al. (1986), in which the DNA strand is more B-like and the RNA strand A-like, with the hybrid taking on characteristics of both A and B (Katayanagi et al., 1992; Federoff et al., 1993). Other techniques, both solution and structural, have shed light on the character of RNA/DNA hybrids. Arnott's fiber experiments were preceded by those of Zimmerman and Pheiffer (1981) who found that depending on its degree of hydration poly rA·oligo dT can adopt two conformations, either A or B. Raman spectroscopy of poly rA·oligo dT shows that the bases are close to the helix axis and that globally rA·dT resembles B-DNA (Benevides & Thomas, 1988). A hybrid DNA/RNA duplex of mixed sequence has been studied by NMR (Salazar et al., 1993;

Federoff et al., 1993) in which the DNA strand differs from both A and B, and is more akin to the heteromerous model of Arnott. The minor groove width in this hybrid is intermediate between that of A- and B-form duplexes. Modeling of RT using this mixed-sequence hybrid as the substrate leads Federoff to postulate that the RNase H pocket needs a more narrow B-like minor groove to function.

Characterization of enzyme-bound RNA/DNA complexes of polymerases by X-ray, NMR, and CD offers further insight into the conformations of both enzyme and substrate duplex. In the Jacobo-Molina et al. (1993) X-ray crystal structure of RT bound to dsDNA, the DNA duplex possesses an A-helical conformation in the polymerase site and a B-helical structure in the RNase H site, connected by a 40° bend at the A−B junction. In the rat DNA pol β complex with DNA (Pelletier et al., 1994), the DNA helix also has an A-conformation at the polymerase site. Oda and co-workers (1993) carried out NMR and CD experiments in which they titrated the nucleic acid substrate with enzyme using three duplexes, DNA/DNA, RNA/RNA, and RNA/DNA. They find that the RNA/DNA duplex binds more tightly than the other duplexes and that the conformation of the enzyme is altered by an *induced fit* to the nucleic acid substrate upon binding. Their CD experiments clearly show that the conformation of the hybrid duplex is altered upon binding, and that this involves an alteration in base stacking. The change in stacking could result in an A−B junction at the bend, of the type shown in Figure 13. It is well-known that a bend arises naturally at an A−B junction, if base pairs remain stacked in an orderly manner across the junction, because of the different inherent inclination angle of base pairs to the helix axis in the A- and B-forms. But no matter what may be concluded about B-helices and A−B junctions, the evidence is clear that the enzyme requires an A-helical conformation *in the polymerase domain*.

How do MPyr and TVin differ from the parent distamycin? MPyr and TVin are both head-to-head bis-linkages of two distamycins, differing only in their linkers. Their molecular structures are compared in Figure 3. Rao et al. (1991) state that, because distamycin ligands bind isohelically to DNA, "the tether should not interfere with the required crescent-shaped conformation of a suitable ligand". The MPyr molecule can swivel at single bonds on either side of the rigid pyridyl−amide linker. Kissinger et al. (1990) propose rotating both distamycin moieties at right angles to a central aryl linker to remove the carbonyl oxygens from close proximity to the aryl ortho hydrogens. Two possibilities exist: One can rotate the central carbonyl groups to the same side of the pyridyl ring or to opposite sides. The latter case is especially favorable, as the overall MPyr bisdistamycin molecule then has a gentle S-shape that can follow the floor of the minor groove as it winds around the enzyme-bound hybrid helix. Although TVin has been shown to bind bidentately to B-DNA (Rao et al., 1991), its linkage gives a different radius of curvature, which is not as compatible with the enzyme−hybrid duplex in the region where MPyr binds.

Where do these bis-distamycins bind? To answer this one has to look at the Jacobo-Molina RT-DNA/DNA X-ray structure and the chemical studies mapping contact regions between the duplex and the enzyme. Metzger et al. (1993) show by hydroxyl radical footprinting that RT protects the region +3 to −15 on the template from the primer 3′ terminus. More recent enzymatic footprinting with DNase
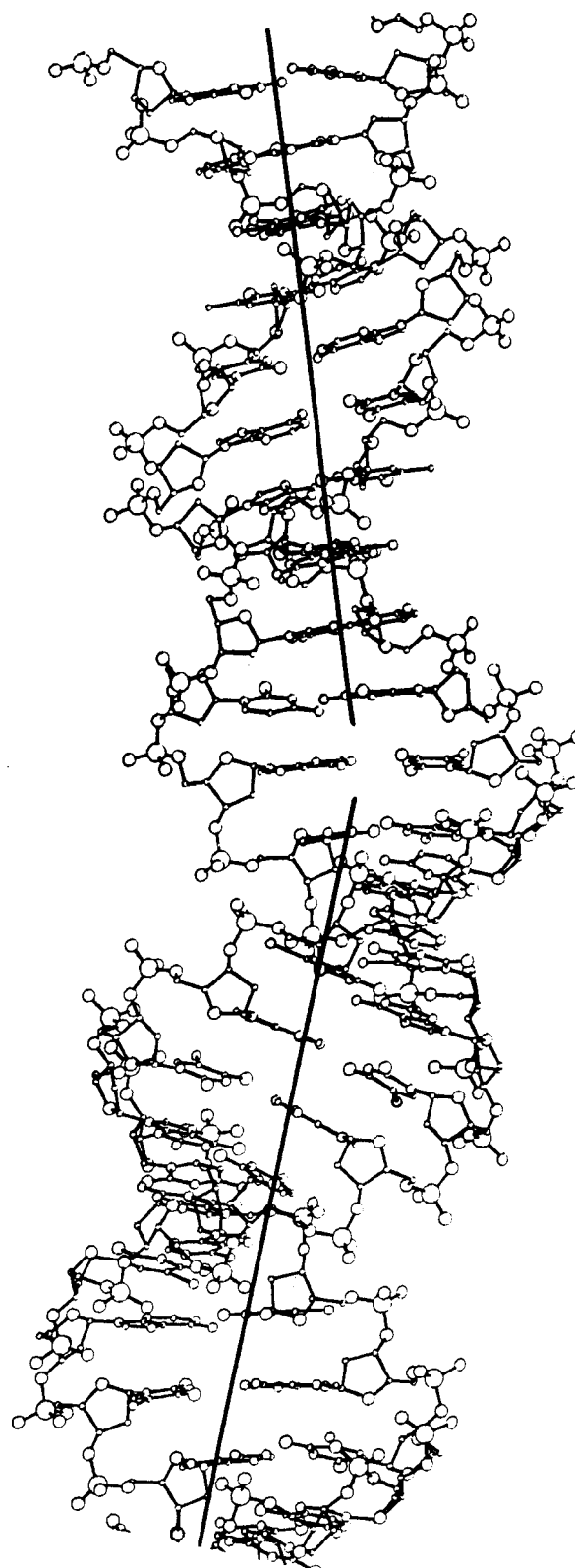

FIGURE 13: Natural bending of helix axis at an A−B junction. The bend arises naturally providing that base pairs are stacked well across the junction, because of the difference in inclination angles of base pairs in the A-helix (below) and B-helix (above). The inclination angle is the angle between the helix axis and a perpendicular to the best plane through the base pair. It is nearly zero for B-DNA, but ranges from 5° to 20° in A-DNA and A-RNA [from Dickerson et al. (1996)].

I (Wohrl et al., 1995) has revealed that RT has an expanded region of interaction to bases +7 to −23, with +3 to −15 contacting the catalytic centers. These studies agree that the

first five to seven base pairs of the template−primer that are in contact with the polymerase domain are in the A-helix form. After a sharp 40° bend in the helix, the remainder of the nucleic acid interaction site is in the B-form (Jacobo-Molina et al., 1993). In the present study, the competitive kinetics of MPyr with regard to primer as substrate imply that both the enzyme primer grip, within the polymerase domain, and the drug bind to the same region of the template−primer.

CD experiments with netropsin and distamycin have shown that these drugs do not bind to A-form helices as such, but induce an A to B (Ivanov et al., 1974; Zimmer, 1975) as well as a Z to B transition (Zimmer et al., 1983) in DNA and RNA helices. Zimmer and co-workers (1982) show that netropsin induces a B-type structure in poly rA·poly dT. MPyr may act by inducing an incorrect, B-helical, conformation at the active site and then binding to it, thus preventing the start of processive addition of nucleotides. It may be that only one of the distamycin ends of MPyr is needed to bind to the TP in the polymerase domain, while the other end may bridge the proposed junction region and extend towards the RNase H domain. The $n+1$ rule determining the size of binding site of a distamycin-like drug (see introduction) indicates at least a ten base pair site, five for each of the two distamycin moieties.

TVin is non-competitive with both primer and nucleotide, indicating that the drug- and enzyme-binding sites on the template−primer do not overlap. There is no dead-end complex, and the enzyme functions at a reduced level. Hence the drug most likely is not binding to TP in contact with the polymerase region, but is positioned somewhere upstream from it, around base pair −10 and beyond. Of course all of this is speculation until NMR or X-ray crystallography can reveal the true positions of the inhibitory drugs, but a reasonable assessment would locate MPyr at or near the primer grip site and TVin farther upstream on the template−primer.

Future Considerations

Because of the limitations in a homopolymeric assay, it would be valuable to confirm these ideas in a heteropolymeric system. The length of starting primer in a homopolymeric assay determines the degree of processivity (Reardon et al., 1991), which affects the turnover frequency, in turn directly affecting the extent of inhibition. Measuring incorporation with acid-precipitable counts (1) does not monitor turnover frequency, only total nucleotide incorporation and (2) limits conclusions to only the polymerization function of RT, leaving the RNase H activity to be investigated. Thus assumptions about conformational changes in regions of the template−primer in contact with the RNase H domain need to be supported with more data.

Focusing on one aspect of HIV replication, RNA-dependent DNA polymerization, presents a new avenue of selectivity. This selectivity is based on the principle of the DNA sequence-reading capability of lexitropsins as well as nucleic acid conformation, and the ability of these drugs to "seek" or induce a conformation in the hybrid duplex. An exciting prospect is the selective targeting of high-consensus genomic regions like the polypurine tract (PPT), which serves as the RNA primer for (+)-strand DNA-directed DNA synthesis. Effective inhibition via lexitropsin binding to the HIV-1 PPT

would present a two-pronged approach to clinical effectiveness. These drugs could be selective on the basis of (1) sequence, $U_5A_4G_4A_4G_6$; high consensus among various strains indicates that the virus cannot afford mutations in this region, and (2) a unique conformation; an RNA primer for DNA synthesis that is not degraded by RT RNase H. Drugs taking advantage of these features could impede mutations that result in drug resistance.

REFERENCES

Andreola, M.-L., Tarrago-Litvak, L., Levina, A. S., Kolocheva, T. I., El Dirani-Diab, R., Jamkovoy, V. I., Khalimskaya, N. L., Barr, P. J., Litvak, S., & Nevinsky, G. A. (1993) *Biochemistry 32*, 3629−3637.

Arcamone, F. (1993) *Il Farmaco 48*, 143−150.

Arcamone, F. M., Animati, F., Barbieri, B., Configliacchi, E., D'Alessio, R., Geroni, C., Giuliani, F. C., Lazzari, E., Menozzi, M., Mongeli, N., Penco, S., & Verini, M. A. (1989) *J. Med. Chem. 32*, 774−778.

Arnott, S., Chandrasekaran, R., Millane, R. P., & Park, H.-S. (1986) *J. Mol. Biol. 188*, 631−640.

Bachur, N. R., Johnson, R., Yu, F., Hickey, R., Applegren, N., & Malkas, L. (1993) *Mol. Pharmacol. 44*, 1064−1069.

Basu, A., Ahluwalia, K. K., Basu, S., & Modak, M. J. (1992) *Biochemistry 31*, 616−623.

Beard, W. A., & Wilson, S. H. (1993) *Biochemistry 32*, 9745−9753.

Benevides, J. M., & Thomas, G. J., Jr. (1988) *Biochemistry 27*, 3868−3873.

Broggini, M., Coley, H. M., Mongelli, N., Pesenti, E., Wyatt, W. D., Hartley, J. A., & D'Incalci, M. (1995) *Nucleic Acids Res. 23*, 81−87.

Buiser, R. G., DeStefano, J. J., Mallaber, L. M., Fay, P. J., & Bambara, R. A. (1991) *J. Biol. Chem. 266*, 13103−13109.

Carteau, S., Mouscadet, J. F., Goulaouic, H., Subra, F., & Auclair, C. (1994) *Biochem. Pharmacol. 47*, 1821−1826.

Chiang, S.-Y., Welch, J., Rauscher, F. J., III, & Beerman, T. A. (1994) *Biochemistry 33*, 7033−7040.

Clark, P. K., Ferris, A. L., Miller, D. A., Hizi, A., Kim, K.-W., Deringer-Boyer, S. M., Mellini, M. L., Clark, A. D., Jr., Arnold, G. F., Lebherz, W. B., III, Arnold, E., Muschik, G. M., & Hughes, S. H. (1990) *AIDS Res. Hum. Retroviruses 6*, 753−764.

De Clercq, E., & Dann, O. (1980) *J. Med. Chem. 23*, 787−795.

Delahunty, M. D., Wilson, S. H., & Karpel, R. L. (1994) *J. Mol. Biol. 236*, 469−479.

Dickerson, R. E., Goodsell, D., & Kopka, M. L. (1996) *J. Mol. Biol. 256*, 108−125.

Divita, G., Muller, U., Immendorfer, U., Gautel, M., Rittinger, K., Restle, T., & Goody, R. S. (1993) *Biochemistry 32*, 7966−7971.

Dorn, A., Affolter, M., Muller, M., Gehring, W. J., & Leupin, W. (1992) *EMBO J. 11*, 279−286.

Federoff, O. Y., Salazar, M., & Reid, B. R. (1993) *J. Mol. Biol. 233*, 509−523.

Feriotto, G., Mischiati, C., & Gambari, R. (1994) *Biochem. J. 299*, 451−458.

Fesen, M. R., Kohn, K. W., Leteurtre, F., & Pommier, Y. (1993) *Proc. Natl. Acad. Sci. U.S.A. 90*, 2399−2403.

Gambari, R., Barbieri, R., Nastruzzi, C., Chiorboli, V., Feriotto, G., Natali, P. G., Giacomini, P., & Arcamone, F. (1991) *Biochem. Pharmacol. 41*, 497−502.

Ghosh, M., Howard, K. J., Cameron, C. E., Benkovic, S. J., Hughes, S. H., & Le Grice, S. F. J. (1995) *J. Biol. Chem. 270*, 7068−7076.

Goodsell, D., & Dickerson, R. E. (1986) *J. Med. Chem. 29*, 727−733.

Guo, D., Gupta, R., & Lown, J. W. (1993) *Anti-Cancer Drug Des. 8*, 369−397.

Heidenreich, O., Kruhoffer, M., Grosse, F., & Eckstein, F. (1990) *Eur. J. Biochem. 192*, 621−625.

Hizi, A., McGill, C., & Hughes, S. H. (1988) *Proc. Natl. Acad. Sci. U.S.A. 85*, 1218−1222.

Huber, H. E., McCoy, J.-M., Seehra, J. S., & Richardson, C. C. (1989) *J. Biol. Chem. 264*, 4669−4678.

Ivanov, V. I., Minchenkova, L. A., Minyat, E. E., Frank-Kamenetski, M. D., & Schyolkina, A. K. (1974) *J. Mol. Biol. 87*, 817−833.

Jacobo-Molina, A., Ding, J., Nanni, R. G., Clark, A. D., Jr., Lu, X., Tantillo, C., Williams, R. L., Kamer, G., Ferris, A. L., Clark, P., Hizi, A., Hughes, S. H., & Arnold, E. (1993) *Proc. Natl. Acad. Sci. U.S.A. 90*, 6320−6324.

Jaju, M., Beard, W. A., & Wilson, S. H. (1995) *J. Biol. Chem. 270*, 9740−9747.

Ji, J., Hoffmann, J.-S., & Loeb, L. (1994) *Nucleic Acids Res. 22*, 47−52.

Katayanagi, K., Miyagawa, M., Matsushima, M., Ishikawa, M., Kanaya, S., Nakamura, H., Ikehara, M., Matsuzaki, T., & Morikawa, K. (1992) *J. Mol. Biol. 223*, 1029−1052.

Khorlin, A. A., Krylov, S. S., Grokhovsky, S. L., Zhuze, A. L., Zasedatelev, A. S., Gursky, G. V., & Gottikh, B. P. (1980) *FEBS Lett. 118*, 311−314.

Kissinger, K. L., Krowicki, K., Dabrowiak, J. C., & Lown, J. W. (1987) *Biochemistry 26*, 5590−5595.

Kissinger, K. L., Dabrowiak, J. C., & Lown, J. W. (1990) *Chem. Res. Toxicol. 3*, 162−168.

Kohlstaedt, L. A., Wang, J., Friedman, J. M., Rice, P. A., & Steitz, T. A. (1992) *Science 256*, 1783−1790.

Kopka, M. L., Yoon, C., Goodsell, D., Pjura, P., & Dickerson, R. E. (1985a) *Proc. Natl. Acad. Sci. U.S.A. 82*, 1376−1380.

Kopka, M. L., Yoon, C., Goodsell, D., Pjura, P., & Dickerson, R. E. (1985b) *J. Mol. Biol. 183*, 553−563.

Krowicki, K., Balzarini, J., De Clercq, E., Newman, R. A., & Lown, J. W. (1988) *J. Med. Chem. 31*, 341−345.

Kruhoffer, M., Urbanke, C., & Grosse, F. (1993) *Nucleic Acids Res. 21*, 3943−3949.

Lown, J. W. (1992) *Antiviral Res. 17*, 179−196.

Lown, J. W., Krowicki, K., Bhat, U. G., Skorobogaty, A., Ward, B., & Dabrowiak, J. C. (1986) *Biochemistry 25*, 7408−7416.

Lown, J. W., Krowicki, K., Balzarini, J., Newman, R. A., & De Clercq, E. (1989) *J. Med. Chem. 32*, 2368−2375.

Luck, G., & Zimmer, C. (1973) *Stud. Biophys. 40*, 9−12.

Majumdar, C., Abbots, J., Broder, S., & Wilson, S. H. (1988) *J. Biol. Chem. 263*, 15657−15665.

Majumdar, C., Stein, C. A., Cohen, J. S., Broder, S., & Wilson, S. H. (1989) *Biochemistry 28*, 1340−1346.

Mazumder, A., Perrin, D. M., McMillen, D., & Sigman, D. S. (1994) *Biochemistry 33*, 2262−2268.

Metzger, W., Hermann, T., Schatz, O., LeGrice, S. F. J., & Heumann, H. (1993) *Proc. Natl. Acad. Sci. U.S.A. 90*, 5909−5913.

Montecucco, A., Fontana, M., Focher, F., Lestingi, M., Spadari, S., & Ciarrocchi, G. (1991) *Nucleic Acids Res. 19*, 1067−1072.

Mortensen, U. H., Stevnsner, T., Krogh, S., Oleson, K., Westergaard, O., & Bonven, B. J. (1990) *Nucleic Acids Res. 18*, 1983−1989.

McHugh, M. M., Sigmund, R. D., & Beerman, T. A. (1990) *Biochem. Pharmacol. 39*, 707−714.

Nevinsky, G. A., Andreola, M.-L., Jamkovoy, V. I., Levina, A. S., Barr, P. J., Tarrago-Litvak, L., Tharaud, D., & Litvak, S. (1992) *Eur. J. Biochem. 207*, 351−358.

Oda, Y., Iwai, S., Ohtsuka, E., Ishikawa, M., Ikehara, M., & Nakamura, H. (1993) *Nucleic Acids Res. 21*, 4690−4695.

Patel, D. J. (1982) *Proc. Natl. Acad. Sci. U.S.A. 79*, 6424−6428.

Patel, P. H., Jacobo-Molina, A., Ding, J., Tantillo, C., Clark, A. D., Jr., Raag, R., Nanni, R. G., Hughes, S. H., & Arnold, E. (1995) *Biochemistry 34*, 5351−5363.

Pelletier, H., Sawaya, M. R., Kumar, A., Wilson, S. H., & Kraut, J. (1994) *Science 264*, 1891−1903.

Puschendorf, B., & Grunicke, H. (1969) *FEBS Lett. 4*, 355−357.

Rao, K. E., Zimmerman, J., & Lown, J. W. (1991) *J. Org. Chem. 56*, 786−797.

Reardon, J. E., Furfine, E. S., & Cheng, N. (1991) *J. Biol. Chem. 266*, 14128−14134.

Rittinger, K., Divita, G., & Goody, R. S. (1995) *Proc. Natl. Acad. Sci. U.S.A. 92*, 8046−8049.

Salazar, M., Fedoroff, O. Y., Miller, J. M., Ribeiro, N. S., & Reid, B. (1993) *Biochemistry 32*, 4207−4215.

Segel, I. H. (1975) in *Enzyme Kinetics: Behavior and Analysis of Rapid Equilibrium and Steady-State Enzyme Systems*, pp 166−169, 184−185, 206−208, John Wiley & Sons, New York.

Shen, L. L., Mitscher, L. A., Sharma, P. N., O'Donnell, T. J., Chu, D. W. T., Cooper, C. S., Rosen & Pernet, A. G. (1989a) *Biochemistry 28*, 3886−3894.

Shen, L. L., Kohlbrenner, W. E., Weigl, D., & Baranowski, J. (1989b) *J. Biol. Chem. 264*, 2973−2978.

Sobol, R. W., Suhadolnik, R. J., Kumar, A., Lee, B. J., Hatfield, D. L., & Wilson, S. H. (1991) *Biochemistry 30*, 10623−10631.

Storl, K., Storl, J., Zimmer, C., & Lown, J. W. (1993) *FEBS Lett. 317*, 157−162.

Subra, F., Mouscadet, J. F., Lavignon, M., Roy, C., & Auclair, C. (1993) *Biochem. Pharmacol. 45*, 93−99.

Ueno, A., Baek, K. H., Jeon, C. J., & Agarwal, K., (1992) *Proc. Natl. Acad. Sci. U.S.A. 89*, 3676−3680.

Van Dyke, M. W., & Dervan, P. B. (1983) *Nucleic Acids Res. 11*, 5555−5563.

Walker, W. L., Kopka, M. L., Filipowsky, M. E., Dickerson, R. E. & Goodsell, D. S. (1995) *Biopolymers 35*, 543−553.

Wahnert, U., Zimmer, C., Luck, G., & Pitra, C. (1975) *Nucleic Acids Res. 2*, 391−404.

Wang, W., & Lown, J. W. (1992) *J. Med. Chem. 35*, 2890−2897.

Wartell, R. M., Larson, J. E., & Wells, R. D. (1974) *J. Biol. Chem. 249*, 6719−6731.

Weislow, O. W., Kiser, R., Fine, D. L., Bader, J., Shoemaker, R. H., & Boyd, M. R. (1989) *J. Natl. Cancer Inst. 81*, 577−586.

Welch, J. J., Rauscher, F. J., III, & Beerman, T. A. (1994) *J. Biol. Chem. 269*, 31051−31058.

Wohrl, B. M., Tantillo, C., Arnold, E., & Le Grice, S. F. J. (1995) *Biochemistry 34*, 5343−5350.

Woynarowski, J. M., Sigmund, R. D., & Beerman, T. A. (1989) *Biochemistry 28*, 3850−3855.

Youngquist, R. S., & Dervan, P. B. (1985) *Proc. Natl. Acad. Sci. U.S.A. 82*, 2565−2569.

Zhan, X., Tan, C.-K., Scott, W. A., Mian, A. M., Downey, K. M., & So, A. G. (1994) *Biochemistry 33*, 1366−1372.

Zimmer, C. (1975) *Prog. Nucleic Acid Res. Mol. Biol. 15*, 285−318.

Zimmer, C., & Luck, G. (1970) *FEBS Lett. 10*, 339−342.

Zimmer, C., Reinert, K. E., Luck, G., Wahnert, U., Lober, G., & Thrum, H. (1971a) *J. Mol. Biol. 58*, 329−348.

Zimmer, C., Puschendorf, B., Grunicke, H., Chandra, P., & Venner, H. (1971b) *Eur. J. Biochem. 21*, 269−278.

Zimmer, C., Kakiuchi, N., & Guschlbauer, W. (1982) *Nucleic Acids Res. 10*, 1721−1732.

Zimmer, C., Marck, C., & Guschlbauer, W. (1983) *FEBS Lett. 154*, 156−160.

Zimmerman, S. B., & Pheiffer, B. H. (1981) *Proc. Natl. Acad. Sci. U.S.A. 78*, 78−82.